Polycrystalline ZnO Nanorods for lasing Applications

NI Maad Tazri[a], OL Muskens[b], MK Shakfa[c], W Maryam[a*]

[a]*School of Physics, Universiti Sains Malaysia, 11800, Penang, Malaysia*
[b]*Physics and Astronomy, Faculty of Physical Sciences and Engineering, University of Southampton, SO17 1BJ, UK*
[c]*Photonics Laboratory, King Abdullah University of Science & Technology (KAUST), Thuwal 23955-6900, Saudi Arabia*
**Corresponding author*

Abstract

Single and double mode random lasing were observed in a polycrystalline ZnO nanorod array. The double mode random lasing showed mode competition when the mode spacing was 2.3 nm or below. Structurally, X-ray diffraction measurements confirmed the formation of the polycrystalline phase and photoluminescence measurements revealed broad visible peak due to point defects, suggesting enhanced oxygen diffusion due to annealing. Our results suggest polycrystalline nanorods obtained by chemical bath deposition as a materials system for obtaining random lasing for applications and devices.

Introduction

The combination of gain and multiple scattering of light in a complex nanostructured media sets the scene for a range of phenomena including amplified stimulated emission and random lasing [1]–[3]. In random lasers, the mirrors of a conventional laser are replaced by the multiple scattering material, which provides gain for a subset of modes in the complex medium. The balance between gain and scattering is subtle and random lasing has been reported in both strongly and weakly scattering systems [4]–[9]. In strongly scattering media, the mode competition generally results in multiple lasing peaks, which interact and compete for gain [10], [11]. However, to realize effective random-lasing-based nanophotonic devices like biosensors, integrated circuits and diagnostics, inevitably it is important to control the random laser. There is no evidence of mode control i.e. limiting the number of lasing modes as well as maintaining consistency in any of these systems.

Several methods of controlling random lasing have been proposed such as by introducing point defects of polymer particles [12], [13], controlling absorption [14], changing the Mie resonances [15], changing transport characteristics [16], waveguiding via electro-optic steering [17] and by introducing some degree of disorder in ZnO nanorod array [18]. The latter also showed that only annealed nanorod arrays can exhibit random lasing behavior. Random lasing in annealed ZnO microstructures in argon atmosphere reported that annealing above 700 °C is required for lasing to occur [19]. All samples however showed crystalline structure for obtaining random lasing.

In this work, single and double mode random lasing emission was obtained from polycrystalline ZnO when annealed at a temperature of 500 ºC. Annealing above this value makes the ZnO nanorods crystalline and lasing characteristics from them are reported in [18]. Random lasing in our current studies was achieved in a thin layer of strongly scattering polycrystalline ZnO nanowires. X-ray diffraction measurements confirm polycrystalline behavior and photoluminescence measurements revealed a broad visible peak possibly from oxygen interstitial due to annealing. Optical scattering properties of the layer are quantified using total transmission and reflection measurements, yielding information on the transport mean free path and showing that the nanowire mat is highly scattering. Single mode lasing emission showed consistency with very small wavelength changes across the sample. For double mode emission, there is a correlation between mode spacing and mode competition.

Methods

ZnO nanostructures were prepared on a pre-coated glass substrate by chemical bath deposition (CBD). All chemicals were used without further purification and the aqueous solution was prepared using deionized water. The glass substrate was pre-coated with a 100 nm thick of ZnO thin film using radio frequency (RF) magnetron sputtering. The substrate undergo annealing treatment at 500 °C for 1 hour in oxygen environment with a flow rate of 3 sl/m. The CBD solution was prepared with a mixture of 0.05 M of zinc nitrate ($Zn(NO_3)_2.6H_2O$) and 0.05 M hexamethylenetetramine (HMT) and the substrate was placed vertically inside the beaker containing the solution. The solution was then heated for 4 hours at 96 ºC. Finally, the sample undergo repeated annealing with the same pre-growth annealing condition. Annealing at a temperature of 500º C results in a polycrystalline state of the nanowire mats.

To investigate the structural properties, field emission scanning electron microscope (FESEM) was used to view the sample's morphology, and X-ray diffraction (XRD) was used to determine the crystal structure of the nanorods. Continuous-wave photoluminescence (cw-PL) measurement using an HeCd laser source operating at 325 nm was utilized to identify optical properties of the sample. In addition, Raman measurements were also performed using an Ar^+ ion laser source to examine the structural properties. Transmittance and reflectance measurements were performed using a Fianium SC-400 supercontinuum light source, whereby total transmission and reflectance spectra are obtained utilizing an integrating sphere. Random lasing measurements were performed using a micro-PL system with an Nd:YAG pulsed laser source operating at 266 nm at 20 KHz repetition rate and with a 550 ps pulse width. The beam spot size was 8 µm in diameter with an incident peak power of 5 MW cm^{-2}. The lasing emission was collected by a spectrometer with resolution of 0.1 nm. All measurements were done in room temperature.

Material Characteristics

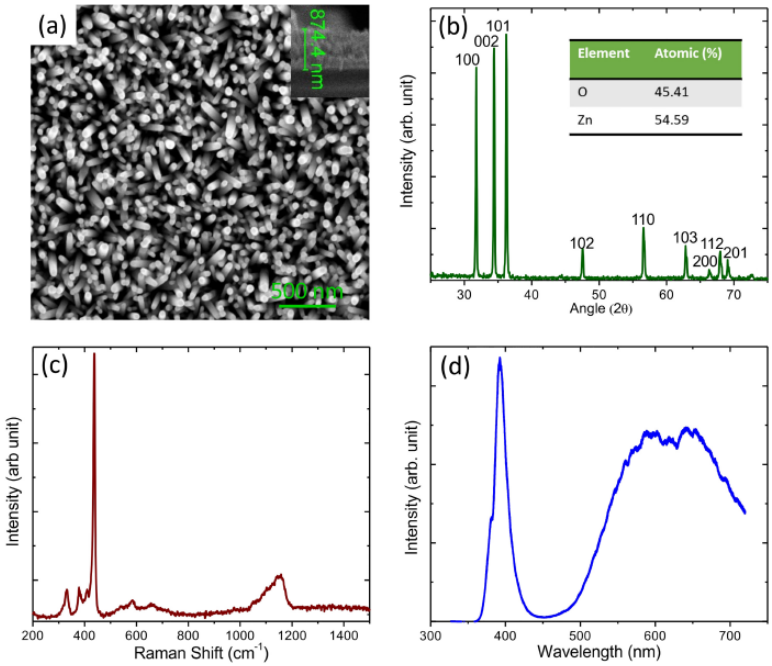

Figure 1: (a) SEM image of ZnO nanorods prepared with insert showing the cross section. (b) XRD spectrum showing three dominant peaks for (100), (002) and (101) planes with insert showing the elements composition of elements obtained from EDX, (c) Raman spectrum with a peak at 435 cm^{-1} corresponding toE_2(H), and (d) cw-PL spectra with near band edge emission centered at 394 nm and emission at 614 nm related to interstitial defects.

Figure 1(a) shows FESEM image of the sample with an insert showing the cross section. A good formation of nanorods with hexagonal wurtzwite structure and a population that spreads equally on the surface are observed. The average diameter of the nanorods is 46 ± 0.3 nm, while the polydisperse distribution of nanowires has a standard deviation of around 10 nm. The population density based on the FESEM image is roughly 255 nanorods/μm^2. Figure 1 (b) shows an XRD spectrum of the sample with polycrystalline structure (JCPDS card no. 36-1451) of hexagonal wurtzite structure. The peak at $2\theta \sim 31°$, 34.4° and 36° correspond to the (100), (002) and (101) planes, respectively. No peaks related to impurites are present. The insert of Fig. 1(b) shows elements' composition in the sample, whereby oxygen contributes 45 %. Figure 1 (c) shows a Raman spectrum obtained from the sample. The $E_2(H)$ peak at 435 cm^{-1} is attributed to hexagonal wurtzite structure and depends on the morphology of nanostructures [20]. The $E_1(L)$ weak peak located at 587 cm^{-1} corresponds to the structural defect including oxygen vacancy [21]. The peak at 332 cm^{-1} is attributed to $A_1(TO)$ due to anisotropy in the force constant, while the peak at378 cm^{-1} is attributed to $E_2(H)$-$E_2(L)$ due to second order Raman spectrum from zone-boundary phonons [22]. The relatively high intensity of the $E_2(H)$ peak can be associated to bond breakage in ZnO due to defects [23]. Figure 1 (d) shows a PL spectrum of the sample; the emission at 394 nm is the near band edge emission (NBE) and the emission centered at 614 nm is typically attributed to O-vacancies and O-interstitial [24]. The green emission is obviously broad due to interstitial and consequently affects the NBE emission [25].

Transport Characteristics

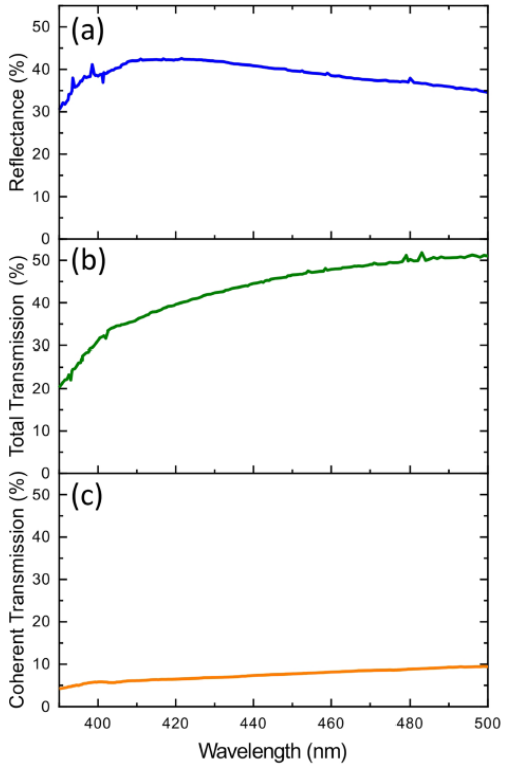

Figure 2: Total reflectance, transmission and coherent transmission (without integrating sphere) of the sample. About 40 % total reflectance and total transmission was obtained and only about 6 % of light coherently transmitted.

High density nanowire mats made from high refractive index materials can exhibit strong optical scattering characteristics [26]. Quantitative studies of the optical response of strongly scattering slabs can be used to extract their multiple scattering characteristics [27], [28]. Figure 2 shows total transmittance and reflectance spectra of the sample collected in an integrating sphere as well as coherent transmission that was obtained without the integrated sphere. Both total reflectance and transmittance spectra show a value of about 40 %

at 420 nm wavelength, indicating that at most 20 % of light is absorbed by the sample in this range. This is an overestimate as some light is trapped by guided modes in the substrate and cannot be collected by the integrating sphere. The amount of light coherently transmitted is 6 ± 1 %. This represents the amount of light not scattered within the structure and may be used to estimate the scattering mean free path using the Beer-Lambert law

$$T_{COH} = e^{-\frac{L}{l_s}} \quad (1)$$

Here T_{COH} is the coherent transmission, L is the nanorod length and l_s is the scattering mean free path. From the coherent transmission, we estimate a value of $l_s = 311 \pm 9$ nm. The transport mean free path can be obtained from the total transmission through the relation [27]

$$T_{TOT} = \frac{1+\tau_e}{L/l_t+2\tau_e}, \quad (2)$$

where τ_e is the extrapolation factor taking into account internal reflections at the boundaries of the layer, and τ_e=2/3 corresponds to perfect index matching [29], [30]. The value of τ_e is of order unity in the case of a ZnO nanowire layer. From the experimental total transmission we find a value of $l_t = 292 \pm 13$ nm, which is of the same order as the scattering mean free path. This value is also of the same order for porous GaP networks [27], a material that was used in other random laser experiments showing spikes [11]. Comparison of the transport mean free paths in other random lasers is provided in Ref. [31]. The overall thickness of the nanowire layers in our sample is around 3 transport mean free paths.

Lasing Characteristics

Optical pumping measurements were performed to study random lasing emission from the sample with a pump beam spot-size of about 8 μm in diameter and an incident peak power of 5 MWcm^{-2}. From FESEM images in Fig 1 (a), about 3200 nanorods are involved in the optical pumping area. Figure 3 (a) shows single mode random lasing at various positions of the pump on the sample. In some positions, double mode lasing is observed as shown in Figure 3 (b). Similar to the single modes, small shifts in wavelengths are observed. However, gain competition between the modes depended on their mode spacing. For example, a mode spacing of 6 nm showed relative intensity of about 1, indicating gain is shared almost equally between the two modes. When the modes are closer to each other, one mode becomes more dominant than the other. Also observed is that the dominant modes have larger FWHM, whereas in the case of equal emission the FWHM of the lasing mode is almost the same. It is possible that having an array of ZnO vertical nanowires for random lasing instead of ZnO spheres or micro resonators, as most reports for random lasing, changes the scattering of the light and hence the gain profile. In this regime, lasing is either single mode or double mode depending on changes of the transport mean free path on the sample. There is also an indication that point defects play a significant role to observe lasing as undoped samples did not show any lasing emission. This may provide a possibility of limiting the number of modes in a random laser as well as for mode-locking applications. A summary of the lasing characteristics is provided in Table 1.

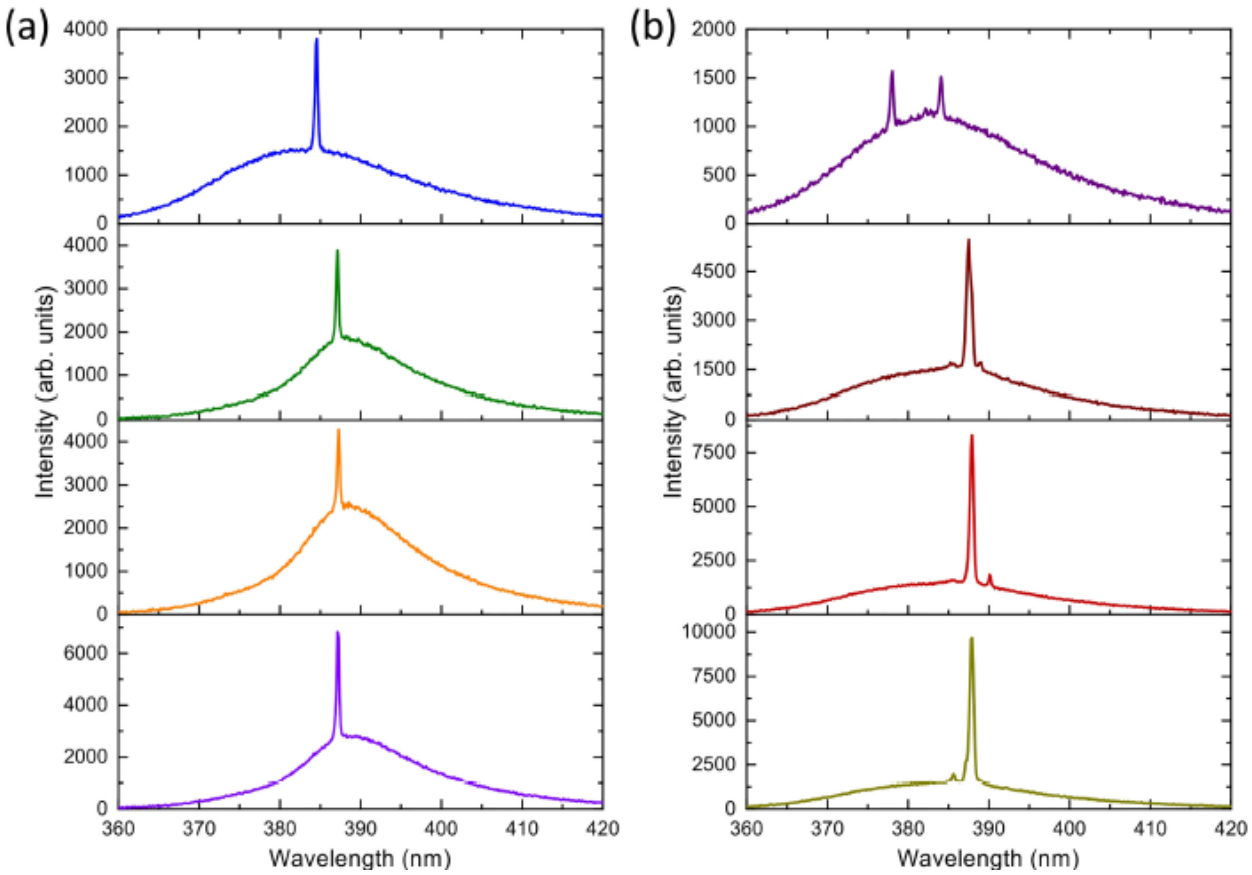

Figure 3: (a) Single mode lasing at different sample's positions. Despite slight shifts in lasing wavelength and varying lasing intensities, all modes maintained FWHM of 0.35 nm at all positions. (b) Double mode random lasing at different positions. When mode spacing was 6 nm (top) equal distribution of gain between modes, whereas in all other cases where mode spacing was 2.3 nm or below, gain competition was observed with one mode dominant over the other.

Table 1: Characteristics of the double lasing modes at specific sample positions.

Position	**λ (nm)**	**FWHM (nm)**	**Δλ (nm)**	**Peak Ratio**
1	378.0 384.0	0.43 0.47	6.0	1.04
2	387.5 385.2	0.76 0.21	2.3	0.31
3	388.0 390.0	0.41 0.29	2.0	0.22
4	385.6 387.9	0.29 0.52	2.3	0.21

The short mean free path of light inside the nanowire mat rules out formation of cavity modes by multiple interference in the slab. To further exclude possible effects from a Fabry-Perot cavity formed by the

nanowire mat we estimate the expected behavior for such a cavity. From simple estimation of the mode spacing in Fabry–Perot systems follows as [32]

$$\Delta\lambda = \lambda^2/(2nL)\,. \quad (3)$$

whereby L is the cavity length, n is the refractive index (2.45) and λ is the resonator wavelength, the mode spacing may be obtained to confirm Fabry–Perot as the lasing mechanism. The average height of the nanorod is 850nm, correspondingly, the mode spacing should be 35.4 nm. However the mode spacings in Fig 3 (b) is only between 2 nm and 6 nm indicating it is not a Fabry–Perot effect. Another possible lasing mechanism is four wave mixing and whispering gallery modes. However the diameter of our nanorods is too small (less than 200 nm) for this to occur especially in its current resonator structure [33]–[35].

The nature of random lasing in polycrystalline ZnO nanowire mats could be further investigated in future studies, for example by looking at the spatial extent of lasing modes [10], [36] and dependence on sample parameters such as thickness of the mat, alignment of the nanowires, and the role of polycrystalline structure. Our work is a first step toward implementation of chemical bath synthesis as a low-cost scalable technique for producing random laser materials, which could spark new applications such as optical sensors [37].

Conclusion

Single and double mode random lasing within the strong scattering regime were observed in thin layers of polycrystalline ZnO nanorods. Double modes showed mode competition when the mode spacing was 2.3 nm and below. When the mode spacing was 6 nm, the two emission peaks show almost equal intensity as well as the same FWHM. Our findings overall demonstrate the possibility of utilizing the scattering regime in ZnO as a control method for random lasers, mode-locking and other lasing applications. It is hoped that these findings spark more experimental and theoretical work in looking at effects of grain and structural boundaries in random lasing.

Acknowledgements

The authors are grateful for partial funding from USM short-term grant [304/PFIZIK/6312155] and from the Global Challenges Research Fund (GCRF) - EPSRC Institutional Sponsorship. The corresponding author also acknowledges Prof Azlan Abdul Aziz for in-kind contribution of the sputtering target.

References

[1] H. Cao, J. Y. Xu, S.-H. Chang, and S. T. Ho, “Transition from amplified spontaneous emission to laser action in strongly scattering media,” *Phys. Rev. E*, vol. 61, no. 2, pp. 1985–1989, Feb. 2000.

[2] C.-S. Wang, T.-Y. Chang, T.-Y. Lin, and Y.-F. Chen, “Biologically inspired flexible quasi-single-mode random laser: An integration of Pieris canidia butterfly wing and semiconductors,” *Sci. Rep.*, vol. 4, no. 1, p. 6736, May 2015.

[3] H. Fujiwara, T. Suzuki, R. Niyuki, and K. Sasaki, “ZnO nanorod array random lasers fabricated by a laser-induced hydrothermal synthesis,” *New J. Phys.*, vol. 18, no. 10, p. 103046, Oct. 2016.

[4] W. Z. W. Ismail, D. Liu, S. Clement, D. W. Coutts, E. M. Goldys, and J. M. Dawes, “Spectral and coherence signatures of threshold in random lasers,” *J. Opt.*, vol. 16, no. 10, p. 105008, Oct. 2014.

[5] X. Meng, K. Fujita, S. Murai, and K. Tanaka, “Coherent random lasers in weakly scattering polymer films containing silver nanoparticles,” *Phys. Rev. A*, vol. 79, no. 5, p. 053817, May 2009.

[6] X. Wu *et al.*, “Random lasing in weakly scattering systems,” *Phys. Rev. A*, vol. 74, no. 5, p. 053812, Nov. 2006.

[7] R. C. Polson and Z. V. Vardeny, “Organic random lasers in the weak-scattering regime,” *Phys. Rev. B*, vol. 71, no. 4, p. 045205, Jan. 2005.

[8] M. Sakai *et al.*, “Random laser action in GaN nanocolumns,” *Appl. Phys. Lett.*, vol. 97, no. 15, p. 151109, Oct. 2010.

[9] C. Tolentino Dominguez, M. de A. Gomes, Z. S. Macedo, C. B. de Araújo, and A. S. L. Gomes, “Multi-photon excited coherent random laser emission in ZnO powders,” *Nanoscale*, vol. 7, no. 1, pp. 317–323, 2015.

[10] K. L. van der Molen, R. W. Tjerkstra, A. P. Mosk, and A. Lagendijk, “Spatial Extent of Random Laser Modes,” *Phys. Rev. Lett.*, vol. 98, no. 14, p. 143901, Apr. 2007.

[11] M. Noginov, J. Novak, and S. Williams, “Modeling of photon density dynamics in random lasers,” *Phys. Rev. A*, vol. 70, no. 6, p. 063810, Dec. 2004.

[12] R. Niyuki, H. Fujiwara, Y. Ishikawa, N. Koshizaki, T. Tsuji, and K. Sasaki, “Toward single-mode random lasing within a submicrometre-sized spherical ZnO particle film,” *J. Opt.*, vol. 18, no. 3, p. 035202, Mar. 2016.

[13] H. Fujiwara, R. Niyuki, Y. Ishikawa, N. Koshizaki, T. Tsuji, and K. Sasaki, “Low-threshold and quasi-single-mode random laser within a submicrometer-sized ZnO spherical particle film,” *Appl. Phys. Lett.*, vol. 102, no. 6, p. 061110, Feb. 2013.

[14] R. G. S. El-Dardiry and A. Lagendijk, “Tuning random lasers by engineered absorption,” *Appl. Phys. Lett.*, vol. 98, no. 16, p. 161106, Apr. 2011.

[15] M. Gaio, M. Peruzzo, and R. Sapienza, “Tuning random lasing in photonic glasses,” *Opt. Lett.*, vol. 40, no. 7, p. 1611, Apr. 2015.

[16] N. Bachelard, P. Gaikwad, R. Backov, P. Sebbah, and R. A. L. Vallée, “Disorder as a Playground for the Coexistence of Optical Nonlinear Effects: Competition between Random Lasing and Stimulated Raman Scattering in Complex Porous Materials,” *ACS Photonics*, vol. 1, no. 11, pp. 1206–1211, Nov. 2014.

[17] G. Assanto, S. Perumbilavil, A. Piccardi, and M. Kauranen, “Electro-optic steering of random laser emission in liquid crystals,” *Photonics Lett. Pol.*, vol. 10, no. 4, p. 103, Dec. 2018.

[18] W. Maryam, N. Fazrina, M. R. Hashim, H. C. Hsu, and M. M. Halim, “Optically driven random lasing in ZnO nanorods prepared by chemical bath deposition,” *Photonics Nanostructures - Fundam. Appl.*, vol. 26, pp. 52–55, Sep. 2017.

[19] T.-F. Dai, W.-C. Hsu, and H.-C. Hsu, “Improvement of photoluminescence and lasing properties in ZnO submicron spheres by elimination of surface-trapped state,” *Opt. Express*, vol. 22, no. 22, p. 27169, Nov. 2014.

[20] E. Muchuweni, T. S. Sathiaraj, and H. Nyakotyo, “Synthesis and characterization of zinc oxide thin films for optoelectronic applications,” *Heliyon*, vol. 3, no. 4, p. e00285, Apr. 2017.

[21] Y. Wang *et al.*, “Effect of different annealing atmospheres on the structure and optical properties of ZnO nanoparticles,” *J. Alloys Compd.*, vol. 485, no. 1–2, pp. 743–746, Oct. 2009.

[22] P. K. Samanta and A. K. Bandyopadhyay, “Chemical growth of hexagonal zinc oxide nanorods and their optical properties,” *Appl. Nanosci.*, vol. 2, no. 2, pp. 111–117, Jun. 2012.

[23] S. A. Bidier, M. R. Hashim, and A. M. Aldiabat, “Effect of Postannealing Treatment on Structural and Optical Properties of ZnO Nanorods Prepared Using Chemical Bath Deposition,” *J. Electron. Mater.*, vol. 46, no. 7, pp. 4455–4462, Jul. 2017.

[24] K. Vanheusden, W. L. Warren, C. H. Seager, D. R. Tallant, J. A. Voigt, and B. E. Gnade, “Mechanisms behind green photoluminescence in ZnO phosphor powders,” *J. Appl. Phys.*, vol. 79, no. 10, pp. 7983–7990, May 1996.

[25] L. L. Yang, Q. X. Zhao, M. Willander, J. H. Yang, and I. Ivanov, “Annealing effects on optical properties of low temperature grown ZnO nanorod arrays,” *J. Appl. Phys.*, vol. 105, no. 5, p. 053503, Mar. 2009.

[26] O. L. Muskens, S. L Diedenhofen, B. C. Kaas, R. E. Algra, E. P.A.M. Bakkers, J. Gómez Rivas, A. Lagendijk, “Large Photonic Strength of Highly Tunable Resonant Nanowire Materials,” *Nano Lett.*, vol. 9, no. 3, pp. 930–934, Mar. 2009.

[27] F. J. P. Schuurmans, “Strongly Photonic Macroporous Gallium Phosphide Networks,” *Science (80-.).*, vol. 284, no. 5411, pp. 141–143, Apr. 1999.

[28] J. Gómez Rivas, R. Sprik, A. Lagendijk, L. D. Noordam, and C. W. Rella, “Static and dynamic transport of light close to the Anderson localization transition,” *Phys. Rev. E*, vol. 63, no. 4, p. 046613, Mar. 2001.

[29] D. J. Durian, “Influence of boundary reflection and refraction on diffusive photon transport,” *Phys. Rev. E*, vol. 50, no. 2, pp. 857–866, Aug. 1994.

[30] J. X. Zhu, D. J. Pine, and D. A. Weitz, “Internal reflection of diffusive light in random media,” *Phys. Rev. A*, vol. 44, no. 6, pp. 3948–3959, Sep. 1991.

[31] K. L. van der Molen, A. P. Mosk, and A. Lagendijk, “Quantitative analysis of several random lasers,” *Opt. Commun.*, vol. 278, no. 1, pp. 110–113, Oct. 2007.

[32] H.-C. Hsu, C.-Y. Wu, and W.-F. Hsieh, “Stimulated emission and lasing of random-growth oriented ZnO nanowires,” *J. Appl. Phys.*, vol. 97, no. 6, p. 064315, Mar. 2005.

[33] G. Grinblat, Y. Li, M. P. Nielsen, R. F. Oulton, and S. A. Maier, “Degenerate Four-Wave Mixing in a Multiresonant Germanium Nanodisk,” *ACS Photonics*, vol. 4, no. 9, pp. 2144–2149, Sep. 2017.

[34] C.-H. Lu, T.-Y. Chao, Y.-F. Chiu, S.-Y. Tseng, and H.-C. Hsu, “Enhanced optical confinement and lasing characteristics of individual urchin-like ZnO microstructures prepared by oxidation of metallic Zn,” *Nanoscale Res. Lett.*, vol. 9, no. 1, p. 178, 2014.

[35] O. Malik, K. G. Makris, and H. E. Türeci, “Spectral method for efficient computation of time-dependent phenomena in complex lasers,” *Phys. Rev. A*, vol. 92, no. 6, p. 063829, Dec. 2015.

[36] J. Fallert, R. J. B. Dietz, J. Sartor, D. Schneider, C. Klingshirn, and H. Kalt, “Co-existence of strongly and weakly localized random laser modes,” *Nat. Photonics*, vol. 3, no. 5, pp. 279–282, May 2009.

[37] S. Caixeiro, M. Gaio, B. Marelli, F. G. Omenetto, and R. Sapienza, “Silk-Based Biocompatible Random Lasing,” *Adv. Opt. Mater.*, vol. 4, no. 7, pp. 998–1003, Jul. 2016.

Author Contribution

WM designed the experiment and performed the optical measurements. MKS performed the lasing measurements. NIMT prepared the sample and OLM designed the transmission and reflectance measurements. All authors prepared the manuscript.